JOURNAL OF MATERIALS SCIENCE 26 (1991) 399–406

Vaporization of glasses in the R_2O–Cs_2O–B_2O_3–SiO_2 (R = Li, Na, K and Rb) system

MITSURU ASANO, TOSHIO HARADA, YASUO MIZUTANI
Institute of Atomic Energy, Kyoto University, Uji, Kyoto 611, Japan

A mass-spectrometric Knudsen effusion method has been used for thermochemical study of the vaporization of alkali borosilicate glasses in the R_2O–Cs_2O–B_2O_3–SiO_2 system, where R = Li, Na, K and Rb. Vapours of $RBO_2(g)$, $CsBO_2(g)$, $R_2(BO_2)_2(g)$ and $RCs(BO_2)_2(g)$ have been identified. Over the glasses in which the molar ratio of $(R_2O + Cs_2O)/B_2O_3$ is slightly larger than unity, vapours of R(g), except for Li(g), have been further observed in the initial stage of heating; over the glass containing lithium, however, the vaporization of Cs(g) has been found. Neither R(g) nor Cs(g) has been identified over the glasses in which the molar ratio is equal to unity. Partial pressures of $CsBO_2(g)$ over the glasses containing lithium and sodium are lower than those with potassium and rubidium, indicating that chemical activities of the $CsBO_2$ pseudo-component in the glasses with lithium and sodium are small. Enthalpies of formation as well as dissociation energies for dimeric vapours of alkali metaborates are not very different from one another, except that the dissociation energies for the dimeric vapours containing lithium are larger than for those containing the other elements.

1. Introduction

The accumulation of knowledge on the vaporization behaviour of borosilicate glasses is very important, because high-level radioactive wastes will be stored after immobilization by incorporating into borosilicate glasses. Among radioactive elements in the wastes, caesium is the most hazardous and its vaporization during vitrification processes may be a serious problem. However, only a few studies have been made on the chemical forms of caesium-containing vapours. Hastie *et al.* [1] have detected $CsBO_2(g)$ by a mass-spectrometric method. Yamanaka *et al.* [2] have found the molar ratio of Cs_2O/B_2O_3 in the volatilized products to be almost unity. The present authors have identified $CsBO_2(g)$ and $LiCs(BO_2)_2(g)$ as caesium-containing vapours by a mass-spectrometric Knudsen effusion method over glasses containing Li_2O and Cs_2O [3], and $CsBO_2(g)$, $Cs_2(BO_2)_2(g)$ and $NaCs(BO_2)_2(g)$ over glasses containing Na_2O and Cs_2O [4]. Furthermore, the present authors [5] have found that the chemical activities of alkali metaborate pseudo-components in borosilicate glasses decrease in going from lithium to caesium; that is, the vaporization of the caesium component is most suppressed thermochemically among alkali components in the borosilicate glasses.

In the present work, vapour species and their partial pressures in equilibrium with borosilicate glasses with compositions $R_2O \cdot 0.15Cs_2O \cdot B_2O_3 \cdot 3SiO_2$ and $0.85R_2O \cdot 0.15Cs_2O \cdot B_2O_3 \cdot 3SiO_2$, where R = Li, Na, K and Rb, have been studied by the mass-spectrometric Knudsen effusion method, and thereby the influences of R elements and the molar ratio $(R_2O + Cs_2O)/B_2O_3$ on the vaporization behaviour of caesium are clarified. Thermochemical quantities for dimeric vapours of alkali metaborates and chemical activities of the caesium component in the glasses have been further determined from the partial pressures of the vapours.

The present authors have already reported the vaporization of glasses in the R_2O–Cs_2O–B_2O_3–SiO_2 system containing lithium [3] and sodium [4]. Consequently, in the present article the results obtained for the glasses with potassium and rubidium will be described in comparison with those for the glasses with lithium [3] and sodium [4].

2. Experimental procedure

Details of the mass spectrometer equipped with a platinum Knudsen cell and the experimental procedure used in the present work have been reported elsewhere [6], and hence only a brief outline is given here.

The platinum cell has an inside diameter of 7 mm and an inside height of 9 mm; the diameter of the effusion orifice is 0.5 mm. Glass samples were prepared from reagent-grade alkali carbonates, boric acid and silicon dioxide by the procedure described in the previous paper [7]. Sample numbers and oxide compositions of the glasses used in the present work and previous publications [3, 4] are shown in Table I.

Each powder sample of about 50 mg was put into the cell and heated under a background pressure of

0022–2461/91 $03.00 + .12

TABLE I Oxide compositions of glasses used in the present work and previous work [3, 4]

Glass	Oxide composition						
	Li_2O	Na_2O	K_2O	Rb_2O	Cs_2O	B_2O_3	SiO_2
20 [3]	1				0.15	1	3
21 [3]	0.85				0.15	1	3
4 [4]		1			0.15	1	3
8 [4]		0.85			0.15	1	3
9 [4]					1	1	3
22			1		0.15	1	3
23			0.85		0.15	1	3
24				1	0.15	1	3
25				0.85	0.15	1	3

less than 2×10^{-5} Pa. Vapours effusing from the orifice were ionized by electron impact with an energy of 53 eV, where the maximum of ion intensity was attained, and ion intensities were measured in the temperature range 781 to 1095 K. Appearance energies for the ions were determined from the ionization efficiency curves by linear extrapolation.

3. Results and discussion

3.1. Vapour species

Ion species identified at 1000 K for glasses 22 to 25 are shown in Table II together with their appearance energies and corresponding vapour species. The assignment of the ion species to the vapour ones was made by a comparison of the ionization behaviour of the vapours over glasses 22 to 25 with that over $KBO_2(s)$ [8], $RbBO_2(s)$ [8], $CsBO_2(s)$ [9] and alkali borosilicate glasses [4, 7].

For glass 22, in which the molar ratio $(K_2O + Cs_2O)/B_2O_3$ is slightly larger than unity, the shape of the ionization efficiency curves of the K^+ ion varies with heating time. The variation of the shape is shown in Fig. 1. Just after the sample temperature is raised to 950 K, no distinct inflexion can be observed in the curve and only a value of $A(K^+) = 4.3 \pm 0.5$ eV is obtained as an appearance energy of the K^+ ion. However, after long heating time (about 3 h) at 950 K, the curve has a clear inflexion at an energy of 9.6 ± 0.5 eV of the impact electron, and the shape is quite similar to that of the K^+ ion for $KBO_2(s)$ [8].

In Fig. 1 is also illustrated the curve for $KBO_2(s)$ [8] as a reference. It has been reported that for $KBO_2(s)$ the K^+ ion with $A(K^+) = 9.6 \pm 0.5$ eV is formed by dissociative ionization from $KBO_2(g)$, and the K^+ ion with $A(K^+) = 4.3 \pm 0.5$ eV by the formation of a positive–negative ion pair from $KBO_2(g)$ [8]. Consequently, it is evident that after a long heating time the K^+ ion for glass 22 is formed from $KBO_2(g)$. Just after heating to 950 K, however, the shape of the curve is different from that after long heating time as well as from that for $KBO_2(s)$ [8], indicating that the vapour species corresponding to the K^+ ion may not be a single species. The agreement of $A(K^+) = 4.3 \pm 0.5$ eV with the ionization energy of K(g), $I(K^+) = 4.341$ eV [10], suggests that the vaporization of K(g) occurs in addition to $KBO_2(g)$ in the initial stage of heating.

For the Cs^+ ion for glass 22, the shape of the ionization efficiency curve even just after heating to 950 K is similar to that for $CsBO_2(g)$ [9]. The result is shown in Fig. 2, where a characteristic inflexion is found at 9.3 ± 0.5 eV. From this result it is obvious that the Cs^+ ion is formed from only $CsBO_2(g)$, and Cs(g) does not vaporize from glass 22.

For glass 23, in which the molar ratio $(K_2O + Cs_2O)/B_2O_3$ is equal to unity, the shape of the ionization efficiency curves of the K^+ ion is quite similar to that for glass 22 after long heating time in Fig. 1, and also the shape for the Cs^+ ion is similar to that in Fig. 2. These results indicate that no vapours of K(g) and Cs(g) are noticeable over glass 23.

Fig. 3 shows the variation of the shape of the ionization efficiency curves of the Rb^+ ion with heating time at 950 K for glass 24, in which the molar ratio $(Rb_2O + Cs_2O)/B_2O_3$ is larger than unity. This variation indicates that the vaporization of Rb(g) occurs from glass 24 in the initial stage of heating. However, from the clear inflexion for the Cs^+ ion similar to that in Fig. 2, one can conclude that Cs(g) does not vaporize even just after heating to 950 K. Neither Rb(g) nor Cs(g) is observed over glass 25, in which the molar ratio $(Rb_2O + Cs_2O)/B_2O_3$ is equal to unity.

The present authors have already studied in detail the vapour species over glasses with the compositions $R_2O \cdot 0.15Cs_2O \cdot B_2O_3 \cdot 3SiO_2$ and $0.85R_2O \cdot 0.15Cs_2O \cdot B_2O_3 \cdot 3SiO_2$ for R = Li [3] and Na [4]. It has been found that, over the glasses with the latter composition, vapours are $RBO_2(g)$, $CsBO_2(g)$, $R_2(BO_2)_2(g)$ and $RCs(BO_2)_2(g)$; the vaporization of Cs(g) is further observed over the glass with the former composition with lithium [3], and Na(g) over the glass with sodium [4] in addition to the above vapours. Thus, the vapour species over the glasses in the R_2O–Cs_2O–B_2O_3–SiO_2 system, where R = Li, Na, K and Rb, are summarized as follows. Over glasses in which the molar ratio $(R_2O + Cs_2O)/B_2O_3$ is equal to unity, the vapours of $RBO_2(g)$, $CsBO_2(g)$, $R_2(BO_2)_2(g)$ and $RCs(BO_2)_2(g)$ are identified. Over glasses, in which the ratio is slightly larger than unity, the vapours of R(g), except for Li(g) are further found in the initial stage of heating; over the glass containing lithium, in contrast to the glasses with sodium, potassium and rubidium, the vaporization of Cs(g) occurs.

The preferential vaporization of R(g) or Cs(g) from glasses with the composition $R_2O \cdot 0.15Cs_2O \cdot B_2O_3 \cdot 3SiO_2$ can be understood from the following thermochemical trend of monomeric vapours of alkali metaborates. The dissociation energies for the bonds between alkali metals and BO_2 in a series of metaborates decrease in going from lithium to sodium and then increase in going to caesium, and the dissociation energy for the Li–BO_2 bond is larger than that for Cs–BO_2 [4]. Hence, the dissociation of the R–BO_2 bond in $RBO_2(g)$, except for R = Li, are preferential compared with that of the Cs–BO_2 bond in $CsBO_2(g)$, and the Cs–BO_2 bond is easily dissociated in comparison with the Li–BO_2 bond in $LiBO_2(g)$. These thermochemical properties explain why the vaporization of R(g), except for Li(g),

TABLE II Appearance energies and vapour species of identified ions

Ion species	Appearance energy (eV)[a]				Vapour species
	Glass 22	Glass 23	Glass 24	Glass 25	
K^+	4.3[b]				K(g)
K^+	4.3; 9.6	4.3; 9.5			KBO_2(g)
KO^+	ND[c]	ND			KBO_2(g)
KBO_2^+	9.1	9.0			KBO_2(g)
$K_2BO_2^+$	9.5	9.5			$K_2(BO_2)_2$(g)
Rb^+			4.2[b]		Rb(g)
Rb^+			4.3; 9.5	4.3; 9.6	$RbBO_2$(g)
RbO^+			ND	ND	$RbBO_2$(g)
$RbBO_2^+$			8.6	8.5	$RbBO_2$(g)
$Rb_2BO_2^+$			9.4	9.4	$Rb_2(BO_2)_2$(g)
Cs^+	3.9; 9.3	3.9; 9.3	3.9; 9.3	3.9; 9.3	$CsBO_2$(g)
CsO^+	ND	ND	ND	ND	$CsBO_2$(g)
$CsBO_2^+$	8.8	8.8	8.7	8.8	$CsBO_2$(g)
B^+	ND	ND	ND	ND	KBO_2(g); $RbBO_2$(g); $CsBO_2$(g)
$KCsBO_2^+$	10.0	10.0			$KCs(BO_2)_2$(g)
$RbCsBO_2^+$			10.0	10.0	$RbCs(BO_2)_2$(g)

[a] Estimated uncertainty is ± 0.5 eV.
[b] Determined in the initial stage of heating to 950 K.
[c] No determination.

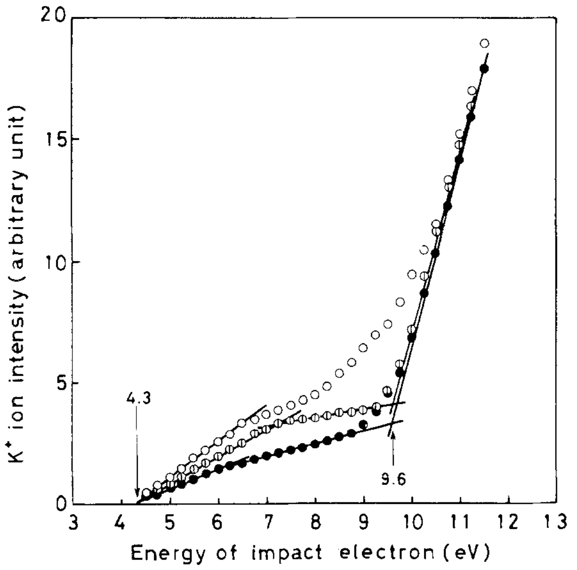

Figure 1 Variation of ionization efficiency curves of K^+ ion for glass 22 with heating time at 950 K; (○) just after heating to 950 K, (◐) after long time at 950 K and (●) the curve for KBO_2(s) [8] as a reference.

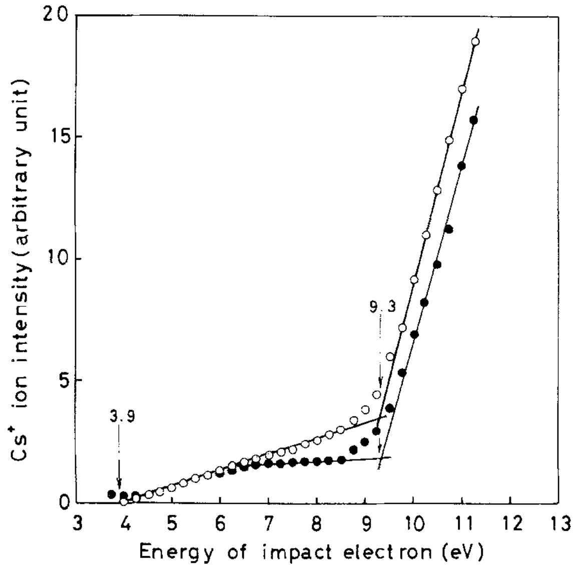

Figure 2 Ionization efficiency curve of Cs^+ ion for glass 22; (○) just after heating to 950 K and (●) the curve for $CsBO_2$(s) [9] as a reference.

is observed over glasses in which the total amount of R_2O plus Cs_2O is in excess of that needed to form imaginary RBO_2 and $CsBO_2$ compounds in the glasses. Similarly, the vaporization of Cs(g), but not Li(g), over the glass with lithium, in which the Li_2O plus Cs_2O content is in excess, can be interpreted from the above thermochemical properties.

3.2. Partial pressures of vapours

The partial pressure p_i of the vapour i was calculated from the equation

$$p_i = k\frac{I_i T}{\sigma_i g_i n_i} \qquad (1)$$

where k is the pressure calibration constant, I_i is the measured ion intensity, T is the sample temperature, σ_i is the relative ionization cross-section, g_i is the gain of the electron multiplier and n_i is the isotopic abundance ratio. The value of k was obtained by the silver reference method. Atomic ionization cross-sections were taken from Mann [11]. Molecular ionization cross-sections were estimated by the method described by Kordis and Gingerich [12] on the assumption that the cross-sections for dissociative ionization are equal to those for simple ionization. The cross-sections for $RbBO_2$(g) and $CsBO_2$(g) were assumed to be equal to the atomic ionization cross-sections for Rb(g) and Cs(g), respectively, because the values calculated by the above method [12] are smaller than those for Rb(g) and Cs(g). Multiplier gains were measured by the pulse counting method [13]. Isotopic abundance

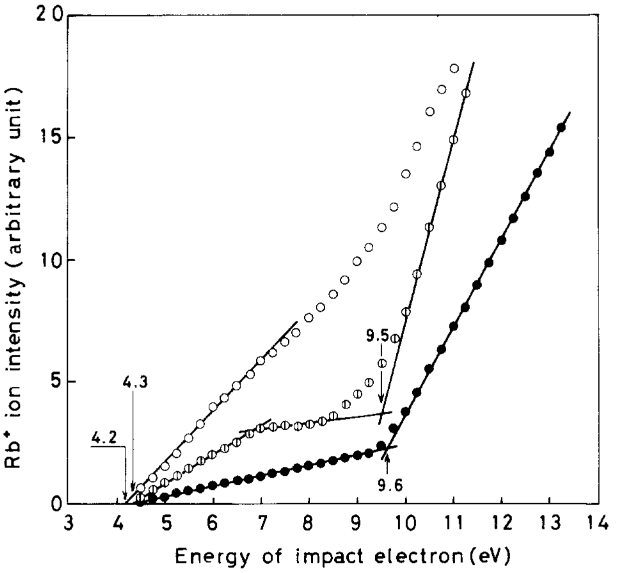

Figure 3 Variation of ionization efficiency curves of Rb^+ ion for glass 24 with heating time at 950 K; (○) just after heating to 950 K, (⦶) after long time at 950 K and (●) the curve for $RbBO_2(s)$ [8] as a reference.

ratios for ^7Li, ^{40}K, ^{85}Rb, ^{11}B and ^{16}O were taken from the literature [10].

On the basis of the assignment of the ion species to the vapour ones in Table II, the partial pressures of the vapours were determined. For example, the partial pressures of $CsBO_2(g)$ were calculated from the intensity measurements of both Cs^+ and $CsBO_2^+$ ions; the contribution of the CsO^+ and B^+ ions was neglected because of their very low intensities.

The determined partial pressures of the vapours over glasses 22 and 23 are shown in Fig. 4 and those over glasses 24 and 25 in Fig. 5. The molar ratios Cs_2O/K_2O and Cs_2O/Rb_2O in the present glasses are about 0.15, but as can be seen in Figs 4 and 5, the partial pressures of $CsBO_2(g)$ are almost equal to those of $KBO_2(g)$ and are slightly lower than those of $RbBO_2(g)$. These results can be understood from the fact that the order of the partial pressures of $RBO_2(g)$ over $RBO_2(s)$ [14] is as follows: $LiBO_2(g) < NaBO_2(g) < KBO_2(g) < RbBO_2(g) < CsBO_2(g)$. Over the present glasses, the vapour of $Cs_2(BO_2)_2(g)$ could not be identified. Consequently, the partial pressures of $Cs_2(BO_2)_2(g)$ were estimated from the thermochemical quantity for $Cs_2(BO_2)_2(g)$ [4] and the measured partial pressures of $CsBO_2(g)$. These estimated values at 1000 K are about 1×10^{-12} Pa over glasses 22 and 23, and about 5×10^{-12} Pa over glasses 24 and 25; that is, these values are far below the sensitivity limit of the mass spectrometer. The ratios of partial pressures $KCs(BO_2)_2(g)/K_2(BO_2)_2(g)$ and $RbCs(BO_2)_2(g)/Rb_2(BO_2)_2(g)$ are about 0.2, being roughly equal to the molar ratios Cs_2O/K_2O and Cs_2O/Rb_2O in these glasses.

Fig. 6 shows a comparison of the partial pressures of $CsBO_2(g)$ over glasses 8 [4], 21 [3], 23 and 25. The partial pressures of $CsBO_2(g)$ are influenced by R_2O coexisting in the present glasses and they are shown in the following order: $Li_2O \simeq Na_2O < K_2O < Rb_2O$;

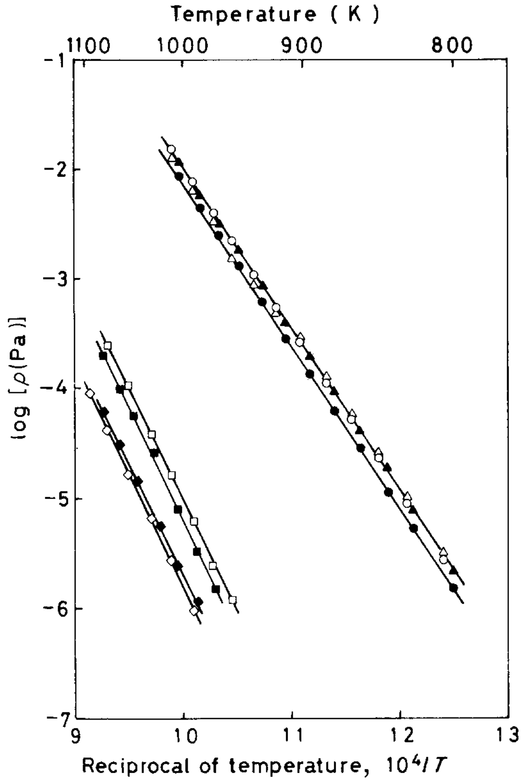

Figure 4 Partial pressures of (○) $KBO_2(g)$, (△) $CsBO_2(g)$, (□) $K_2(BO_2)_2(g)$ and (◇) $KCs(BO_2)_2(g)$ over glass 22 and those of (●) $KBO_2(g)$, (▲) $CsBO_2(g)$, (■) $K_2(BO_2)_2(g)$ and (◆) $KCs(BO_2)_2(g)$ over glass 23.

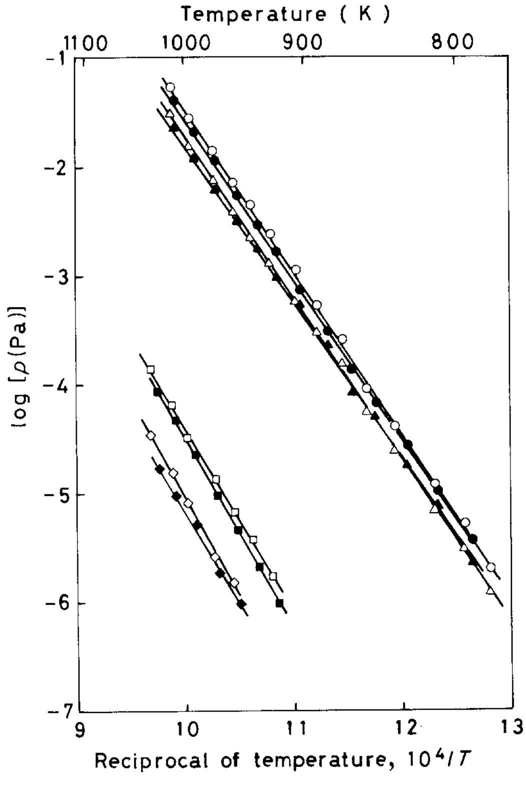

Figure 5 Partial pressures of (○) $RbBO_2(g)$, (△) $CsBO_2(g)$, (□) $Rb_2(BO_2)_2(g)$ and (◇) $RbCs(BO_2)_2(g)$ over glass 24 and those of (●) $RbBO_2(g)$, (▲) $CsBO_2(g)$, (■) $Rb_2(BO_2)_2(g)$ and (◆) $RbCs(BO_2)_2(g)$ over glass 25.

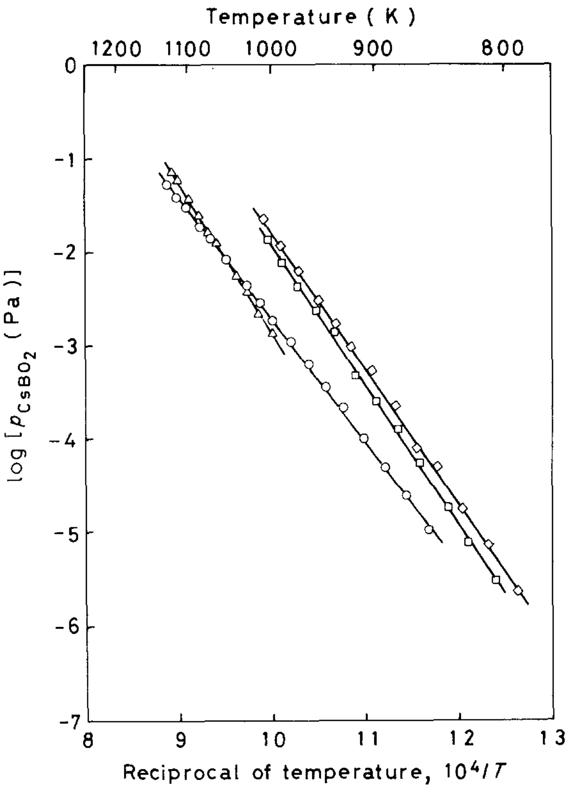

Figure 6 Partial pressures of $CsBO_2(g)$ over glasses (△) 8 [4], (○) 21 [3], (□) 23 and (◇) 25.

in other words, the chemical activity of the caesium component in the glasses follows the above order. This shows that the vaporization of hazardous caesium is most suppressed thermochemically in the glasses containing Li_2O and Na_2O. The activities of the alkali components will be discussed in section 3.4. below.

Least-squares equations fitted to the partial pressures of vapours over glasses 22 to 25 are listed in Table III. Here, uncertainties quoted in the equations are the standard deviations of coefficients. However, uncertainties in the partial pressures arise from the uncertainties in the measurements of ion intensities and also from those in the conversion of intensities to partial pressures. From experimental and other probable uncertainties, the uncertainties in the partial pressures are estimated to be $\Delta \log p_i = \pm 0.2$.

3.3. Thermochemical quantities for dimerization reaction

From the measurements of partial pressures, free energies of dimerization reaction at 1000 K were determined for

$$2RBO_2(g) = R_2(BO_2)_2(g) \qquad (2)$$

$$RBO_2(g) + CsBO_2(g) = RCs(BO_2)_2(g) \qquad (3)$$

The results are shown in Table IV. The value of the

TABLE III Least-squares equations $\log p = A - (10^3\,B/T)$ for partial pressures of vapours[a]

Glass	Vapours	Temperature range (K)	A	B
22	$KBO_2(g)$	807 to 1012	12.98 ± 0.14	14.96 ± 0.13
	$CsBO_2(g)$	807 to 1012	11.86 ± 0.19	13.98 ± 0.17
	$K_2(BO_2)_2(g)$	957 to 1076	15.30 ± 0.20	20.33 ± 0.20
	$KCs(BO_2)_2(g)$	991 to 1095	14.74 ± 0.20	20.57 ± 0.21
23	$KBO_2(g)$	800 to 1006	12.69 ± 0.09	14.83 ± 0.08
	$CsBO_2(g)$	800 to 1006	12.91 ± 0.15	14.84 ± 0.13
	$K_2(BO_2)_2(g)$	972 to 1080	15.57 ± 0.39	20.79 ± 0.40
	$KCs(BO_2)_2(g)$	988 to 1080	14.34 ± 0.11	20.05 ± 0.11
24	$RbBO_2(g)$	781 to 1012	13.63 ± 0.12	15.08 ± 0.10
	$CsBO_2(g)$	781 to 1012	13.20 ± 0.10	14.92 ± 0.09
	$Rb_2(BO_2)_2(g)$	906 to 1033	12.64 ± 0.15	17.04 ± 0.15
	$RbCs(BO_2)_2(g)$	957 to 1033	13.24 ± 0.54	18.27 ± 0.54
25	$RbBO_2(g)$	791 to 1008	13.45 ± 0.09	14.96 ± 0.08
	$CsBO_2(g)$	791 to 1008	12.85 ± 0.18	14.60 ± 0.16
	$Rb_2(BO_2)_2(g)$	920 to 1026	12.76 ± 0.18	17.26 ± 0.17
	$RbCs(BO_2)_2(g)$	953 to 1026	12.09 ± 0.61	17.27 ± 0.60

[a] Unit of pressure is Pa.

TABLE IV Free energies at 1000 K ($\Delta G^\circ_{r,1000}$) and third-law enthalpies at 0 K ($\Delta H^\circ_{r,0}$) for dimerization reaction

Reaction	Glass	$\Delta G^\circ_{r,1000}$ (kJ mol^{-1})	$\Delta H^\circ_{r,0}$ (kJ mol^{-1})
$2LiBO_2(g) = Li_2(BO_2)_2(g)$	21 [3]	− 132.6 ± 7.1	− 298.8 ± 9.0
$2NaBO_2(g) = Na_2(BO_2)_2(g)$	8 [4]	− 114.6 ± 7.1	− 282.7 ± 9.0
$2KBO_2(g) = K_2(BO_2)_2(g)$	23	− 77.8 ± 7.1	− 244.0 ± 9.0
$2RbBO_2(g) = Rb_2(BO_2)_2(g)$	25	− 67.5 ± 7.1	− 219.8 ± 9.0
$2CsBO_2(g) = Cs_2(BO_2)_2(g)$	9 [4]	− 53.5 ± 7.1	− 210.0 ± 9.0
$LiBO_2(g) + CsBO_2(g) = LiCs(BO_2)_2(g)$	21 [3]	− 102.5 ± 5.9	− 262.9 ± 8.1
$NaBO_2(g) + CsBO_2(g) = NaCs(BO_2)_2(g)$	8 [4]	− 92.2 ± 5.9	− 248.9 ± 8.1
$KBO_2(g) + CsBO_2(g) = KCs(BO_2)_2(g)$	23	− 62.6 ± 5.9	− 223.4 ± 8.1
$RbBO_2(g) + CsBO_2(g) = RbCs(BO_2)_2(g)$	25	− 59.1 ± 5.9	− 209.6 ± 8.1

free energy for Equation 2 decreases numerically by the change from R = Li to R = Cs. This indicates that, when the partial pressures of $RBO_2(g)$ are almost equal, the partial pressure of $Cs_2(BO_2)_2(g)$ is the smallest. This is the reason why $K_2(BO_2)_2(g)$ and $Rb_2(BO_2)_2(g)$ are found, while the observation of $Cs_2(BO_2)_2(g)$ is very difficult over the present glasses. Similarly, the values of free energies in Table IV show that $RCs(BO_2)_2(g)$ is more easily identified than $Cs_2(BO_2)_2(g)$.

Third-law enthalpies of dimerization reaction at 0 K for Equations 2 and 3 were further determined from the partial pressures and free energy functions for $RBO_2(g)$ [15, 16], $R_2(BO_2)_2(g)$ [17] and $RCs(BO_2)_2(g)$. Here, the free-energy functions for $RCs(BO_2)_2(g)$ were estimated by averaging those for $R_2(BO_2)_2(g)$ [17] and $Cs_2(BO_2)_2(g)$ [17]. In Table IV are also shown the third-law enthalpies of dimerization reaction for Equations 2 and 3. The combination of the enthalpies of dimerization reaction with the enthalpies of formation for $RBO_2(g)$ [18] and $CsBO_2(g)$ [18] yields the enthalpies of formation for $R_2(BO_2)_2(g)$ and $RCs(BO_2)_2(g)$, and further combination with the enthalpies of formation for R(g) [15], Cs(g) [15] and $BO_2(g)$ [15] gives the dissociation energies for the bonds between alkali metals and BO_2 in $R_2(BO_2)_2(g)$ and $RCs(BO_2)_2(g)$. These values are shown in Table V. It is known that, for monomeric vapours of alkali metaborates, the enthalpies of formation as well as the dissociation energies decrease numerically in going from lithium to sodium and then increase in going to caesium; that is, the values for $NaBO_2(g)$ are minima in both cases [4]. For dimeric vapours of alkali metaborates, however, a similar tendency is not obvious. One can only recognize that the dissociation energies for the dimeric vapours containing lithium are larger than for those containing the others.

3.4. Chemical activities of alkali components in glasses

The compositions of the glasses used in the present work and previous ones [3, 4] are shown in Table I in terms of the oxide components. However, it is evident from a Raman spectrometric study [19] that all the alkali ions are associated with borate units in alkali borosilicate glasses where the molar ratio R_2O/B_2O_3 is less than unity. A similar conclusion has been reached from a nuclear magnetic resonance study [20]. This preferential association of the alkali ions with borate units, but not with silicate units, may be confirmed from the fact that the free energy of formation for $RBO_2(s)$ [15] is lower than half of that for $R_2SiO_3(s)$ [15]. Consequently, in the present glasses with the oxide composition $0.85R_2O \cdot 0.15Cs_2O \cdot B_2O_3 \cdot 3SiO_2$, all the R^+ and Cs^+ ions are probably associated with borate units. Furthermore, the vapours of $RBO_2(g)$ and $CsBO_2(g)$ are observed over the glasses. Thus, according to Wenzel and Sanders [21], the composition can be rewritten by using alkali pseudo-components, the chemical formulae of which are the same as those of the vapours, as $1.7RBO_2 \cdot 0.3CsBO_2 \cdot 3SiO_2$. In this case, the chemical activity of a given alkali pseudo-component in the glass can be determined from the ratio between the partial pressure of the corresponding vapour over the glass and that over a pure compound of the same chemical formula as the vapour. For example, the activity and the activity coefficient for the $CsBO_2$ pseudo-component were calculated from the equation

$$\gamma_{CsBO_2} = a_{CsBO_2}\left(\frac{1}{X_{CsBO_2}}\right) = \frac{p_{CsBO_2}}{p^{\circ}_{CsBO_2}}\left(\frac{1}{X_{CsBO_2}}\right) \quad (4)$$

Here a is the chemical activity, γ is the activity coefficient, X is the molar fraction, p is the partial pressure over the glass and p° is the partial pressure over $CsBO_2(s)$ [14].

TABLE V Third-law enthalpies of formation ($\Delta H^{\circ}_{f,0}$) and dissociation energies (D°_0) for dimeric vapours of alkali metaborates at 0 K

Vapour	Glass	$\Delta H^{\circ}_{f,0}$ (kJ mol^{-1})	D°_0 (kJ mol^{-1})
$Li_2(BO_2)_2(g)$	21 [3]	-1595.0 ± 11.0	1347.4 ± 20.4
$Na_2(BO_2)_2(g)$	8 [4]	-1555.9 ± 13.6	1202.9 ± 21.6
$K_2(BO_2)_2(g)$	23	-1593.2 ± 20.1	1204.3 ± 26.6
$Rb_2(BO_2)_2(g)$	25	-1575.8 ± 41.6	1171.2 ± 44.9
$Cs_2(BO_2)_2(g)$	9 [4]	-1584.0 ± 41.6	1171.4 ± 45.1
$LiCs(BO_2)_2(g)$	21 [3]	-1598.0 ± 22.1	1267.9 ± 28.1
$NaCs(BO_2)_2(g)$	8 [4]	-1572.5 ± 22.4	1189.1 ± 28.1
$KCs(BO_2)_2(g)$	23	-1585.0 ± 23.8	1184.2 ± 29.3
$RbCs(BO_2)_2(g)$	25	-1574.6 ± 29.8	1160.0 ± 34.3

Table VI shows the chemical activities, molar fractions and activity coefficients of alkali pseudo-components in the glasses with compositions $1.7RBO_2 \cdot 0.3CsBO_2 \cdot 3SiO_2$ at 1000 K. The present authors [5] have already reported that, in the glasses with composition $2R'BO_2 \cdot 3SiO_2$ (R′ = Li, Na, K, Rb and Cs), the activity and the activity coefficient for $R'BO_2$ decrease in going from $LiBO_2$ to $CsBO_2$. As can be seen in Table VI, these values for RBO_2 in the present glasses decrease in the above order, too.

An interpretation of the variation of the activity coefficient of RBO_2 can be made as follows. Richardson [22] has proposed that, in ionic melts in the MO–YO–SiO_2 system, the activity coefficient of the MO component may be described as

$$RT \ln \gamma_{MO} = \alpha_{MY}X_{YO}^2 + \alpha_{MSi}X_{SiO_2}^2 + (\alpha_{MY} + \alpha_{MSi} - \alpha_{YSi})X_{YO}X_{SiO_2} \quad (5)$$

Here α_{MY} is the energy of interaction between M^{2+} and Y^{2+} ions through M^{2+}–O–Y^{2+}. Thus, in the present glasses with the composition $1.7RBO_2 \cdot 0.3CsBO_2 \cdot 3SiO_2$, the activity coefficient of the RBO_2 component is probably given by

$$RT \ln \gamma_{RBO_2} \propto \beta_{RCs}X_{CsBO_2}^2 + \alpha_{RSi}X_{SiO_2}^2 + (\beta_{RCs} + \alpha_{RSi} - \alpha_{CsSi})X_{CsBO_2}X_{SiO_2} \quad (6)$$

Here β_{RCs} is the energy of interaction between R^+ and

TABLE VI Chemical activities (α), molar fractions (X) and activity coefficients (γ) of pseudo-components (underlined) in glasses at 1000 K

Glass	Pseudo-component	α	X	γ
21 [3]	$1.7\underline{LiBO_2}\cdot 0.3CsBO_2\cdot 3SiO_2$	0.16	0.34	0.47
8 [4]	$1.7\underline{NaBO_2}\cdot 0.3CsBO_2\cdot 3SiO_2$	4.4×10^{-2}	0.34	0.13
23	$1.7\underline{KBO_2}\cdot 0.3CsBO_2\cdot 3SiO_2$	3.4×10^{-2}	0.34	0.10
25	$1.7\underline{RbBO_2}\cdot 0.3CsBO_2\cdot 3SiO_2$	1.6×10^{-2}	0.34	4.7×10^{-2}
21 [3]	$1.7LiBO_2\cdot 0.3\underline{CsBO_2}\cdot 3SiO_2$	1.4×10^{-4}	0.06	2.3×10^{-3}
8 [4]	$1.7NaBO_2\cdot 0.3\underline{CsBO_2}\cdot 3SiO_2$	9.1×10^{-5}	0.06	1.5×10^{-3}
23	$1.7KBO_2\cdot 0.3\underline{CsBO_2}\cdot 3SiO_2$	7.9×10^{-4}	0.06	1.3×10^{-2}
25	$1.7RbBO_2\cdot 0.3\underline{CsBO_2}\cdot 3SiO_2$	1.2×10^{-3}	0.06	2.0×10^{-2}

Cs^+ ions through R^+–BO_2–Cs^+. The energies of anion–anion interaction are assumed to be probably constant irrespective of R. Consequently, for discussion of the tendency of the variation of γ_{RBO_2}, the energies of cation–cation interactions alone may be considered as given above.

Since $X^2_{SiO_2}$ in Equation 6 is the largest among molar fractions in the present glasses, then Equation 6 is written approximately as

$$RT\ln\gamma_{RBO_2} \propto \alpha_{RSi}X^2_{SiO_2} \qquad (7)$$

As mentioned already, the order of the activity coefficient of RBO_2 is $\gamma_{LiBO_2} > \gamma_{NaBO_2} > \gamma_{KBO_2} > \gamma_{RbBO_2}$. To give this order, the value of α_{RSi} should be in the order $\alpha_{LiSi} > \alpha_{NaSi} > \alpha_{KSi} > \alpha_{RbSi}$. The variation of α_{RSi} could not be found in the literature. However, it has been pointed out that for alkaline earths the value of α_{MSi} becomes more negative with an increase of the radius of M^{2+} [22]. In fact, values of $\alpha_{MgSi} = -67$ kJ and $\alpha_{CaSi} = -134$ kJ have been reported [23]. These values suggest that the order of α_{RSi} is that given above. That is, the variation of γ_{RBO_2} can be explained from the energies of interaction between R^+ and Si^{4+} ions in the glasses.

The chemical activity and the activity coefficient of the $CsBO_2$ component are also affected by RBO_2 coexisting in the present glasses, and they are in the following order: $LiBO_2 \simeq NaBO_2 < KBO_2 < RbBO_2$ as shown in Table VI. As with γ_{RBO_2}, the activity coefficient of the $CsBO_2$ component may be written as

$$RT\ln\gamma_{CsBO_2} \propto \beta_{RCs}X^2_{RBO_2} + \alpha_{CsSi}X^2_{SiO_2} + (\beta_{RCs} + \alpha_{CsSi} - \alpha_{RSi})X_{RBO_2}X_{SiO_2} \qquad (8)$$

The relation $|\alpha_{MgCa}| > |\alpha_{MgSi} - \alpha_{CaSi}|$ is obtained for alkaline earths, because of $\alpha_{MgCa} = -100$ kJ [23]. Consequently, $|\beta_{RCs}| > |\alpha_{CsSi} - \alpha_{RSi}|$ probably holds. From this relation, Equation 8 is approximated as

$$RT\ln\gamma_{CsBO_2} \propto \beta_{RCs}X^2_{RBO_2} + \alpha_{CsSi}X^2_{SiO_2} + \beta_{RCs}X_{RBO_2}X_{SiO_2} \qquad (9)$$

To give the above order of γ_{CsBO_2}, the value of β_{RCs} should be in the following order: $\beta_{LiCs} \simeq \beta_{NaCs} < \beta_{KCs} < \beta_{RbCs}$, because α_{CsSi} is constant. The value of $\Delta H^\circ_{r,0}$ for Equation 3 is shown in Table IV to be in the order $LiBO_2 < NaBO_2 < KBO_2 < RbBO_2$. This relation probably holds in the interactions between the RBO_2 and $CsBO_2$ pseudo-components in the glasses. Consequently, from the order of $\Delta H^\circ_{r,0}$, it is very likely that the value of β_{RCs} varies in the above order. This explains the variation of γ_{CsBO_2} with RBO_2.

4. Conclusions

The vaporization behaviour was studied for alkali borosilicate glasses in the R_2O–Cs_2O–B_2O_3–SiO_2 system, where R = Li, Na, K and Rb. Vapours of RBO_2(g), $CsBO_2$(g), $R_2(BO_2)_2$(g) and $RCs(BO_2)_2$(g) are identified. Furthermore, in the initial stage of heating, R(g) is found over glasses in which the molar ratio $(R_2O + Cs_2O)/B_2O_3$ is slightly larger than unity, except that Cs(g) is observed over the glass containing lithium. No vaporization of R(g) and Cs(g) occurs over glasses in which the ratio is equal to unity. Partial pressures of $CsBO_2$(g) are influenced by R_2O coexisting in the present glasses, and they are shown to be in the order $Li_2O \simeq Na_2O < K_2O < Rb_2O$. This indicates that chemical activities of the $CsBO_2$ pseudo-component in the glasses vary in the above order. Enthalpies of formation as well as dissociation energies for dimeric vapours are not very different from one another, except that the dissociation energies for the dimeric vapours containing lithium are larger than those containing the other elements. The results obtained in the present work are very useful for predicting the vaporization behaviour of alkali elements, particularly caesium, from borosilicate glasses incorporated with actual high-level radioactive wastes at high temperatures in vitrification processes.

Acknowledgements

The authors are grateful to Professor Dr E. Ichise, Department of Metallurgy, Faculty of Engineering, Kyoto University, for valuable discussions. This study was partially supported by the Grants-in-Aid for Scientific Research and for Installation from the Ministry of Education, Science and Culture, Japan.

References

1. J. W. HASTIE, E. R. PLANTE and D. W. BONNEL, Report NBSIR-83-2731 (National Institute of Standards and Technology, Washington, DC, 1983).
2. H. YAMANAKA, R. TERAI and S. HARA, *Osaka Kogyo Gijutsu Shikenjo Kiho (Bull. Govt. Inst., Osaka)* **34** (1983) 228.
3. M. ASANO, T. HARADA and Y. MIZUTANI, *High Temp. Sci.* to be published.

4. M. ASANO, T. KOU and Y. YASUE, *J. Non-Cryst. Solids* **92** (1987) 245.
5. M. ASANO, T. KOU and Y. MIZUTANI, *ibid.* **112** (1989) 381.
6. M. ASANO and Y. YASUE, *J. Nucl. Mater.* **138** (1986) 65.
7. M. ASANO and T. KOU, *Phys. Chem. Glasses* **30** (1989) 39.
8. M. ASANO, Y. YASUE and K. KUBO, *Bull. Inst. Atom. Energy, Kyoto Univ.* **66** (1984) 39.
9. M. ASANO, Y. YASUE and K. KUBO, *J. Nucl. Sci. Technol.* **21** (1984) 614.
10. D. E. GRAY, "American Institute of Physics Handbook", 3rd Edn (McGraw-Hill, New York, 1972) p. 7-6.
11. J. B. MANN, in "Recent Developments in Mass Spectroscopy", edited by K. Ogata and T. Hayakawa (University of Tokyo press, Tokyo, 1970) p. 814.
12. J. KORDIS and K. A. GINGERICH, *J. Chem. Phys.* **58** (1973) 5141.
13. M. ASANO, H. KIMURA and K. KUBO, *Mass Spectros.* **27** (1979) 157.
14. M. ASANO. T. KOU, Y. YASUE and H. NAKAGAWA, *Bull. Inst. Atom. Energy, Kyoto Univ.* **73** (1988) 51.
15. R. D. STULL and H. PROPHET, "JANAF Thermochemical Tables", 2nd Edn (US Printing Office, Washington, DC, 1971), Supplements 1974, 1975, 1978, 1982 and 1985.
16. Y. YASUE, M. ASANO and K. KUBO, *Bull. Inst. Atom. Energy, Kyoto Univ.* **65** (1984) 49.
17. A. V. GUSAROV, A. V. MAKAROV and O. T. NIKITIN, *Zh. Fiz. Khim.* **51** (1977) 525.
18. Y. YASUE and M. ASANO, *Bull. Inst. Atom. Energy, Kyoto Univ.* **67** (1985) 48.
19. T. FURUKAWA and W. B. WHITE, *J. Mater. Sci.* **16** (1981) 2689.
20. Y. H. YUN and P. T. BRAY, *J. Non-Cryst. Solids* **27** (1978) 363.
21. J. T. WENZEL and D. M. SANDERS, *Phys. Chem. Glasses* **23** (1982) 47.
22. F. D. RICHARDSON, "Physical Chemistry of Melts in Metallurgy", Vol. 1 (Academic, London, 1974) p. 202.
23. S. BAN-YA and M. HINO, *Tetsu-to-Hagane* (*J. Iron and Steel Inst. Jpn*) **73** (1987) 476.

Received 31 July 1989
and accepted 19 February 1990